machines

MDPI

Article

Formation and Change of Unmanned Ground Vehicles under Formation Change Influence Factor

Tianhao Gong, Jianhui Song * and Yang Yu

School of Automation and Electrical Engineering, Shenyang Ligong University, Shenyang 110000, China
* Correspondence: songjianhui@sylu.edu.cn

Abstract: Traditional formation control methods are widely used in the field of unmanned ground vehicle formation, but they lack mechanisms with which to effectively cope with complex terrains that occur during movement. In order to better improve the adaptation and coping ability of an unmanned ground vehicles (UGVs) fleet to complex terrains, this paper proposes a formation change influence factor to solve the UGVs formation and formation change problem. First, this paper adopts the leader–follower method with more flexible control to design the formation controller and derives a control law that can make the formation system stable so as to ensure that the fleet maintains the preset formation during movement. After that, this paper combines formation geometry change and dynamic adjustment to build a formation change library. The formation change influence factor is used to drive the fleet to choose the appropriate formation change strategy in the formation change library to ensure the fleet can safely pass the complex terrains. The experimental results show that, compared with the traditional formation method, the UGVs formation and change method using the formation change influence factor can flexibly and efficiently cope with various complex terrains while maintaining stability within the fleet, effectively improving the safety of the UGVs fleet and the possibility of practical application.

Keywords: unmanned ground vehicles; formation change; formation change influence factor

check for updates

Citation: Gong, T.; Song, J.; Yu, Y. Formation and Change of Unmanned Ground Vehicles under Formation Change Influence Factor. *Machines* **2022**, *10*, 872. https://doi.org/10.3390/machines10100872

Academic Editor: Sam-Sang You

Received: 22 August 2022
Accepted: 25 September 2022
Published: 28 September 2022

Publisher's Note: MDPI stays neutral with regard to jurisdictional claims in published maps and institutional affiliations.

Copyright: © 2022 by the authors. Licensee MDPI, Basel, Switzerland. This article is an open access article distributed under the terms and conditions of the Creative Commons Attribution (CC BY) license (https://creativecommons.org/licenses/by/4.0/).

1. Introduction

In recent years, with the rapid development of robotics and communication networks, multi unmanned ground vehicles (UGVs) cooperative systems have started to attract more researchers' attention. Such systems make human–vehicle cooperation as well as vehicle–vehicle cooperation possible. Compared to individual vehicles, multiple vehicles mean that they can be faster, more flexible and more reliable in accomplishing their tasks. Likewise, this means that multi-vehicle systems place higher demands on cooperative control than single vehicles. For a large collection of vehicles, a common collaborative task that is currently applied in practice is the formation control of UGVs.

The formation control problem can be mainly summarized as follows: (1) generation of formation shapes; (2) formation tracking; (3) reconfiguration and selection of formations; and (4) task assignment in formations [1].

Generally, a number of vehicles are required to form a fixed formation to travel to a certain place for reconnaissance surveillance, positioning guidance, material transportation and other tasks [2]. In the execution of the task, each vehicle within the team has its own group and number, and needs to be in its respective corresponding position in a unified formation. There exists the potential of travelling over certain complex terrain; these terrains usually have a serious impact on the expected formation that the fleet wishes to maintain, or may even lead to the formation's breakdown, making the fleet unable to maintain the original geometric configuration. In order to ensure the successful completion of the mission, the unmanned fleet needs to have a certain ability to cope with the possible formation breakup in addition to the ability to ensure that a certain formation

can be maintained for continuous marching, which is generally made possible by making appropriate formation changes to avoid risks according to the actual conditions. Therefore, the formation tracking and the reconfiguration and selection of formation in the above formation control problem have become hot issues in the field of UGVs formation in recent years.

Formation tracking is generally performed by designing formation controllers to achieve a stable fleet to maintain a preset formation operation [3]. The most commonly used formation control strategies include a virtual structure, behavior-based approaches, the leader–follower approach, graph-based approach, and artificial potential field approach.

In the work of L Yang and Y Jia [4], a distributed D-type iterative learning scheme is developed for multi-agent systems with unknown nonlinear dynamics. This presents an efficient solution to the multi-agent formation control problem. The switching time and order of this learning scheme varies according to the actual trajectory of the agents to ensure that a pre-defined formation is always formed after some iterations. In the work of Giroung and Dongkyoung [5], a decentralized behavior-based formation control algorithm is designed to accomplish the formation task using only the relative position in-formation between robots and obstacles and between neighboring robots. Sida et al. [6] present a hybrid formation control of wheeled mobile robots (WMRs), which is based on model predictive control (MPC) and adaptive terminal sliding mode control (ATSMC). The MPC is used to ensure the stability of the formation, while the ATSMC is used to compensate for external interference. Park B. S and Yoo S. J. [7] investigated a connectivity-preserving obstacle avoidance problem to track uncertain multiple non-holonomic mobile robots with communication and sensing range constraints based on guaranteed performance of leader–follower formations. To address the shortcomings of the unmanned vehicle formation method, Zhi Y. C. et al. [8] proposes an unmanned vehicle formation method based on the improved pigeon flock algorithm with the pilot following method. There are certain limitations when using the traditional pigeon flock algorithm for formation, so an initial solution is provided at the beginning of the algorithm to improve the computational efficiency, and the corresponding weight indicator is added to the geomagnetic operator of the algorithm to improve the planning efficiency of the algorithm in the overall path. Wang X. S. and Cao G. H. [9] study the unmanned vehicle formation control problem in which the unmanned vehicle leader has various unknowns such as unknown linear velocity, angular velocity and unknown upper bound. The unmanned vehicle formation control problem is transformed into the unmanned vehicle consistency problem by transformation. After that, by establishing a time-varying feedback control method, the unmanned vehicle consistency control problem is solved, and then the unmanned vehicle formation control is realized. Shao J et al. [10] propose and solve the problem of asynchronous tracking control for a multi-agent system with uncertain inputs on a switching band signed graph. Shoja S et al. [11] exploit an adaptive controller with consideration of the nonlinear dynamics and the unknown parameters, while the graph and Lyapunov theories are applied to ensure the formation stability. Ali Z. A., Israr A., Alkhammash E. H., et al. [12] provide an adaptive hybrid controller for controlling formations of leader–follower configurations of multiple unmanned aerial vehicles (UAVs) with communication delays. Li D et al. [13] define a multilayer formation control problem and present a model-based control method to implement multilayer formations where the formation configuration can be constant or time-varying. Wang B., Ashrafiuon H. and Nersesov S. [14] solve the distributed leader–follower simultaneous formation stabilization and tracking control problem for a heterogeneous planar underdriven vehicle network with no global position measurement of the follower. The vehicles in the network are modeled as generic 3-DOF planar rigid bodies with two control inputs and are allowed to have either identical or dissimilar dynamics. Liu X et al. [15] designed a formation potential field that combines multiple local attraction potential fields with multiple local repulsion potential fields for multi-agent formation control. The objective is to control a set of agents to automatically generate and maintain a specific formation while avoiding internal collisions and collisions with

spatial constraints. H Sang et al. [16] proposed a novel deterministic algorithm, i.e., the Multi-sub-target Artificial Potential Field (MTAPF) based on improved APF to ensure the optimality, rationality, and path continuity of fleet formation trajectories of unmanned surface vehicles (USVs). MTAPF can greatly reduce the probability of USVs falling into local minima and help USVs escape local minima by switching target points.

In general, several of the formation methods mentioned above have some formation change capability, i.e., the fleet is transformed into a certain defined geometric formation by changing the geometric relationship between vehicle positions. However, traditional formation controllers are designed with the primary goal of maintaining a stable formation; rarely is the problem of fleet formation change specifically considered, and the formation change capability of these methods themselves is limited. This implies that the formation of UGVs under traditional methods cannot appear to affect the stability of the formation during the movement. When encountering unknown and complex road environments, these methods lack corresponding coping mechanisms, thus very easily leading to breakup of the UGVs' formation. In addition, the UGVs fleet in practical applications has a larger number of vehicles compared to the general fleet research object. The increase in number makes it more difficult to plan the path and change the formation in real time during the driving process. How to ensure the overall stability of the fleet while flexibly changing the formation to cope with the unknown terrain environment is now a priority for the decision-making level of the UGVs fleet.

Compared with other methods, the distributed control of the leader–follower method is more flexible and makes it easier to realize the formation change of the geometric relationship. However, the communication between vehicles under this method is focused on that between the leader and the follower, which makes the decisions made by the leader critical for the whole fleet. After receiving the road condition information sent by the sensors, the decision-making layer of the leader can be processed quickly and provide the appropriate solution, which has an important impact on the overall safe and stable operation of the fleet.

Therefore, in order to simultaneously solve the formation problem and the strain problem for the complex terrain of the UGVs fleet, this paper proposes a formation change method for UGVs under the effect of the formation change influence factor. Firstly, the formation controller is designed using the leader–follower method to ensure that the fleet can maintain a fixed formation normally and steadily in the absence of obstacles. After that, the formation geometry change and dynamic adjustment are combined to establish the formation change library, and the formation change of the fleet is based on the formation change library. The formation change influence factor is introduced in the formation controller, the road condition information returned by the sensors is processed centrally, and the formation change is judged accordingly. The generated influence factors are transmitted to the controllers of each vehicle using shop floor communication to drive the controllers to make adjustments and finally make the fleet formation change.

2. Methods

2.1. Formation Controller Design

As the most widely used formation method [17,18], the leader–follower method of distributed control is more flexible and makes it easier to achieve formation changes in geometric relations. This paper utilizes this method as the base method for controller design. The geometric relationship between a leader and a follower is provided in Figure 1.

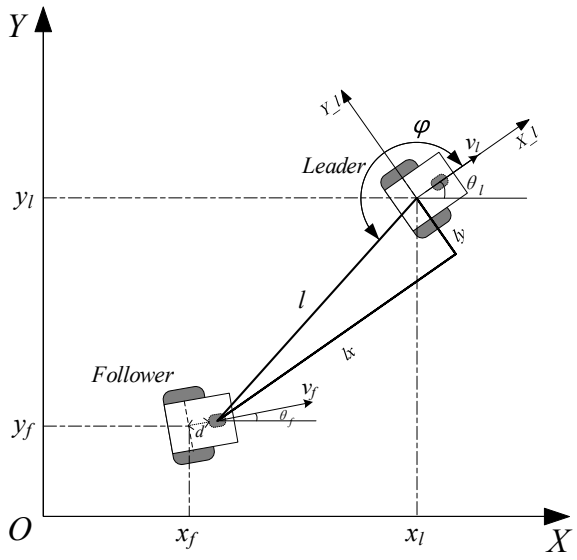

Figure 1. Vehicle models under the leader- follower method.

In Figure 1, the $X-Y$ coordinate system is the world coordinate system, and (x_l, y_l) and (x_f, y_f) represent the positions of the leader and the follower under this coordinate system, respectively. v_l and v_f represent the respective linear velocities, and θ_l and θ_f represent the forward direction angles of both, respectively. d represents the distance between the wheel axle and the guide wheel. l represents the distance between the midpoint of the leader wheel axle and the follower guide wheel. The coordinate system $X_l - Y_l$ is established with the midpoint of the leader wheel axle as the coordinate origin, the forward direction of the leader vehicle as the X-axis direction, and the Y-axis direction perpendicular to the forward direction. l_x and l_y represent the relative distance from the follower to the leader in the X_l, Y_l directions, and φ represents the relative angle between the leader and the follower.

If (l, φ) is deterministic, given the information of the position of the leader, the follower can follow the leader at a fixed angle and distance. Therefore, we assume that the desired relative distance and relative angle between the leader and the follower are (l', φ'), and both can maintain a fixed formation during travel as long as the conditions $l \to l', \varphi \to \varphi'$ are satisfied. In order to avoid singularities in the formation controller, [19] we proposed vehicle modeling and controller design in the Cartesian coordinate system. According to the geometric relations in Figure 1, it is known that

$$l_y = (x_l - x_f - d\cos\theta_f)\sin\theta_l - (y_l - y_f - d\sin\theta_f)\cos\theta_l \tag{1}$$

$$l_x = -(x_l - x_f - d\cos\theta_f)\cos\theta_l - (y_l - y_f - d\sin\theta_f)\sin\theta_l \tag{2}$$

Taking the derivative of l_x, we obtain

$$\begin{aligned} \dot{l_x} = &-(\dot{x_l} - \dot{x_f} + d\omega_f \sin\theta_f)\cos\theta_l + (x_l - x_f - d\cos\theta_f)\omega_l \sin\theta_l \\ &-(\dot{y_l} - \dot{y_f} + d\omega_f \cos\theta_f)\sin\theta_l - (y_l - y_f - d\sin\theta_f)\omega_l \cos\theta_l \end{aligned} \tag{3}$$

Substituting (1) into (3), we obtain

$$\begin{aligned} \dot{l_x} &= l_y\omega_l - \dot{x_l}\cos\theta_l - \dot{y_l}\sin\theta_l + \dot{x_f}\cos\theta_l + \dot{y_f}\sin\theta_l - d\omega_f \sin(\theta_f - \theta_l) \\ &= l_y\omega_l - v_l + \dot{x_f}\cos\theta_l + \dot{y_f}\sin\theta_l - d\omega_f \sin(\theta_f - \theta_l) \end{aligned} \tag{4}$$

where $v_l = \dot{x_l}\cos\theta_l + \dot{y_l}\sin\theta_l$ is the linear velocity of the leader car. $\omega_l = \dot{\theta_l}$ and $\omega_f = \dot{\theta_f}$ denote the respective angular velocities of the leader and the follower, respectively.

Let the forward direction angular error $e_\theta = \theta_f - \theta_l$, then $\theta_l = \theta_f - e_\theta$. Substituting this into (4), we obtain

$$\begin{aligned} \dot{l_x} &= l_y\omega_l - v_l + \dot{x_f}\cos(\theta_f - e_\theta) + \dot{y_f}\sin(\theta_f - e_\theta) - d\omega_f \sin e_\theta \\ &= l_y\omega_l - v_l + \dot{x_f}\cos\theta_f \cos e_\theta + \dot{x_f}\sin\theta_f \sin e_\theta \\ &\quad + \dot{y_f}\sin\theta_f \cos e_\theta - \dot{y_f}\cos\theta_f \sin e_\theta - d\omega_f \sin e_\theta \\ &= l_y\omega_l - v_l + (\dot{x_f}\cos\theta_f + \dot{y_f}\sin\theta_f)\cos e_\theta + \\ &\quad (\dot{x_f}\sin\theta_f - \dot{y_f}\cos\theta_f)\sin e_\theta - d\omega_f \sin e_\theta \end{aligned} \tag{5}$$

According to the non-complete constraint for UGVs:

$$\dot{x_f}\sin\theta_f - \dot{y_f}\cos\theta_f = 0 \tag{6}$$

Substituting (6) into (5), we obtain

$$\dot{l_x} = l_y\omega_l - v_l + v_f\cos e_\theta - d\omega_f \sin e_\theta \tag{7}$$

where $v_f = \dot{x_f}\cos\theta_f + \dot{y_f}\sin\theta_f$ is the linear velocity of the following car. Similarly, we can obtain

$$\dot{l_y} = -l_x\omega_l + v_f\sin e_\theta + d\omega_f \sin e_\theta \tag{8}$$

The kinematic model of the leader–follower system is as follows:

$$\begin{cases} \dot{l_x} = l_y\omega_l - v_l + v_f\cos e_\theta - d\omega_f \sin e_\theta \\ \dot{l_y} = -l_x\omega_l + v_f\sin e_\theta + d\omega_f \sin e_\theta \\ \dot{e_\theta} = \omega_f - \omega_l \end{cases} \tag{9}$$

where (v_f, ω_f) is the angular and linear velocities of the follower, which are the inputs to the control, and (v_f, ω_f) is the angular and linear velocities of the leader, which are given either as a constant value or as a time-varying function.

In the above, it has been shown that if it is desired to keep a fixed formation between the follower and the leader so that they move together, the conditions $l \to l', \varphi \to \varphi'$ need to be satisfied. Due to the saturation of the motor on the UGVs, v_l and ω_l are bounded, and their first-order derivatives are also bounded. Since (l_x, l_y) is the projection of l in the X_l,Y_l direction, combined with the kinematic model of the system, our control objective is as follows: given the input (v_f, ω_f), make $l_x \to {l_x}', l_y \to {l_y}', \varphi \to \varphi'$. According to this requirement, the design of the formation controller is initiated.

First, it follows from the geometric relationship that

$${l_x}' = l'\cos\varphi' \tag{10}$$

$${l_y}' = l'\sin\varphi' \tag{11}$$

Derivation of (10) and (11) leads to

$$\dot{{l_x}'} = \dot{l'}\cos\varphi' - l'\dot{\varphi'}\sin\varphi' \tag{12}$$

$$\dot{{l_y}'} = \dot{l'}\sin\varphi' + l'\dot{\varphi'}\cos\varphi' \tag{13}$$

Suppose $e_x = {l_x}' - l_x$ and $e_y = {l_y}' - l_y$. We can obtain

$$\begin{aligned} \dot{e_x} &= \dot{{l_x}'} - \dot{l_x} \\ &= \dot{l'}\cos\varphi' - l'\dot{\varphi'}\sin\varphi' - l_y\omega_l + v_l - v_f\cos e_\theta + d\omega_f \sin e_\theta \\ &= \dot{l'}\cos\varphi' - l'\dot{\varphi'}\sin\varphi' - \left({l_y}' - e_y\right)\omega_l + v_l - v_f\cos e_\theta + d\omega_f \sin e_\theta \end{aligned} \tag{14}$$

Similarly, we can obtain that

$$\dot{e_y} = \dot{l'} \sin \varphi' + l' \dot{\varphi'} \cos \varphi' + (l_x{}' - e_x)\omega_l - v_f \sin e_\theta - d\omega_f \sin e_\theta \tag{15}$$

The error model of the system is

$$\begin{cases} \dot{e_x} = \dot{l'} \cos \varphi' - l' \dot{\varphi'} \sin \varphi' - (l_y{}' - e_y)\omega_l + v_l - v_f \cos e_\theta + d\omega_f \sin e_\theta \\ \dot{e_y} = \dot{l'} \sin \varphi' + l' \dot{\varphi'} \cos \varphi' + (l_x{}' - e_x)\omega_l - v_f \sin e_\theta - d\omega_f \sin e_\theta \\ \dot{e_\theta} = \omega_f - \omega_l \end{cases} \tag{16}$$

Because the fleet needs to maintain a fixed geometric structure during its movement, the expected values l' and φ' are constants, $\dot{l'} = 0$ and $\dot{\varphi'} = 0$. At this point, the error model of the system can be expressed as

$$\begin{cases} \dot{e_x} = e_y\omega_l - l'\omega_l \sin \varphi' + v_l - v_f \cos e_\theta + d\omega_f \sin e_\theta \\ \dot{e_y} = -e_x\omega_l + l'\omega_l \cos \varphi' - v_f \sin e_\theta - d\omega_f \sin e_\theta \\ \dot{e_\theta} = \omega_f - \omega_l \end{cases} \tag{17}$$

We assume that

$$g_1 = v_l - l'\omega_l \sin \varphi' \tag{18}$$

$$g_2 = l'\omega_l \cos \varphi' \tag{19}$$

It is obvious that both g_1 and g_2 are known. Substituting them into (17) yields

$$\begin{cases} \dot{e_x} = e_y\omega_l - v_f \cos e_\theta + d\omega_f \sin e_\theta + g_1 \\ \dot{e_y} = -e_x\omega_l - v_f \sin e_\theta - d\omega_f \sin e_\theta + g_2 \\ \dot{e_\theta} = \omega_f - \omega_l \end{cases} \tag{20}$$

Let $z = \begin{bmatrix} e_x & e_y \end{bmatrix}^T$, $u = \begin{bmatrix} v_f & u_f \end{bmatrix}^T$, $u = \begin{bmatrix} v_f & u_f \end{bmatrix}^T$. Write (20) in matrix form:

$$\dot{z} = Az + Bu + g \tag{21}$$

where $A = \begin{bmatrix} 0 & \omega_l \\ -\omega_l & 0 \end{bmatrix}$, $B = \begin{bmatrix} -\cos e_\theta & d \sin e_\theta \\ -\sin e_\theta & -d \sin e_\theta \end{bmatrix}$.

Since $\det(B) \neq 0$, input–output linearization can be performed. Let $-Kz = Az + Bu + g$ and solve for

$$u = B^{-1}(-Kz - Az - g) \tag{22}$$

where $K = [k_1 \; k_2]^T > 0$.

From the above equation, the final control law can be derived as

$$v_f = (k_1 e_x + e_y\omega_l + g_1) \cos e_\theta - (-k_2 e_y + e_x\omega_l - g_2) \sin e_\theta \tag{23}$$

$$\omega_f = \frac{1}{d}\left[-(k_1 e_x + e_y\omega_l + g_1) \sin e_\theta - (-k_2 e_y + e_x\omega_l - g_2) \cos e_\theta\right] \tag{24}$$

where k_1 and k_2 are adjustable parameters.

Consider the formation control problem of two tricycle mobile robots shown in Figure 1. For any given bounded and sufficiently smooth leader path, a constant relative distance and an arbitrary smooth relative angle between follower and leader can be obtained asymptotically by the proposed control laws (23) and (24), and the whole system will be stable. The proof is provided in the literature [20].

2.2. Formation Change Library

As the most commonly used formation control method for UGVs today, the use of the leader–follower method results in excellent formation control that allows the fleet of

UGVs to steadily maintain a desired formation while moving. When we wish to change the formation of the fleet, this can be achieved by simply changing the relative position between each follower and the leader. However, UGVs fleets based on the leader–follower method are not equipped to handle complex terrains. In order to move faster and safer through such complex terrains, the fleet needs to incorporate formation change abilities to deal with these situations.

There are two ways in which the UGVs formation structure can be transformed. One is to completely change the geometry of the formation so that it changes from a particular original geometry to another new formation shape altogether [21–23], as shown in Figure 2. Such a change often requires the reallocation of the positions of the vehicles within the fleet, which is a common formation change in the commonly used UGVs formation control methods. Such a formation change requires that it be completed at a faster rate during the fleet movement. This is to ensure that subsequent fleet movements are not affected. Therefore, finding a more stable and faster formation change is essential for the safe and stable operation of the fleet.

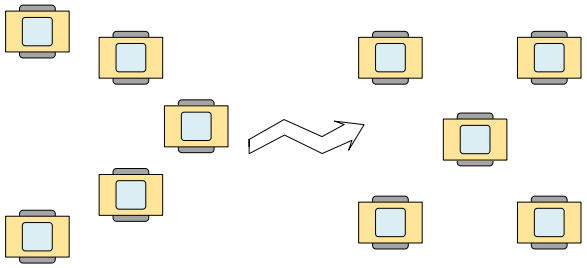

Figure 2. Schematic diagram of geometric change of the formation.

Another way of changing UGVs' formation is to adjust the vehicle spacing within the fleet according to the environmental requirements; this change is generally called the dynamic adjustment of the formation [24–26]. By scaling the vehicle fleet appropriately, it can be adapted to the environment. Compared with the complete change of the formation geometry, this adjustment is faster and more adaptable to different terrain environments. Figure 3 outlines the transformation method of dynamic fine tuning. When the sides of the road become narrow, the leader reduces the vehicle spacing within the convoy in order to ensure the safety of the convoy, which can be achieved by changing the (l', φ') of each follower. However, the reduction in the vehicle spacing undoubtedly increases the possibility of collisions between vehicles within the convoy. This has an adverse effect on the safe operation of unmanned convoys. Therefore, when the road continues to become clear, the navigator orders the remaining followers to resume their original formation.

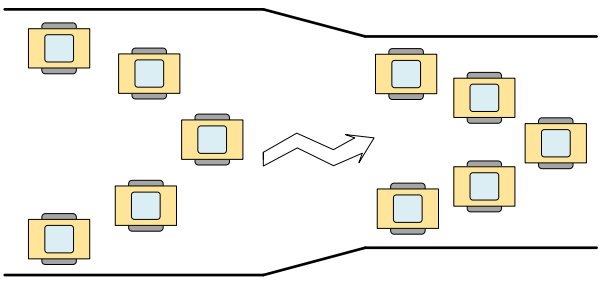

Figure 3. Schematic diagram of dynamic adjustment of the formation.

Although dynamic adjustment is more flexible, it cannot handle all situations. Considering the different complex terrain, one formation change method is not sufficient. If we want the fleet to change the formation structure flexibly according to the current terrains, we need to combine formation geometry change and formation dynamic adjustment to

build a formation change library. The specific change strategies included in the formation change library used in this paper are shown in Figure 4 below.

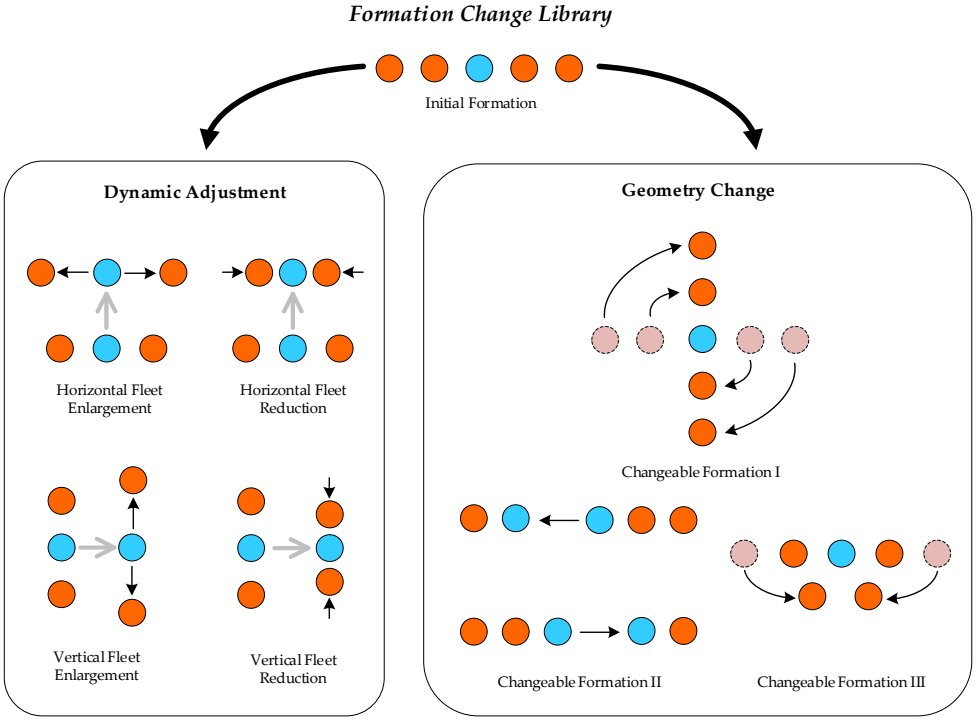

Figure 4. The formation change library of the UGVs fleet.

The blue dots in Figure 4 indicate the leaders of the fleet and the remaining red dots indicate the followers; the dashed circles indicate the initial position of vehicles in the fleet, and the arrows indicate the movement direction of vehicles when the fleet changes formation. This formation change library contains a base formation and a variety of changeable formations. The base formation is the pre-defined formation that needs to be maintained when the UGVs fleet starts moving; this formation depends on what kind of task one wants the fleet to accomplish. In addition, the library needs to contain information about the various formations, such as (1) the formation geometry, (2) the way the formation is generated, (3) the logic of the formation change, and so on.

(1) The formation geometry will tell the UGVs system's decision-making layer the size of the formation, the maximum and minimum acceptable distance between vehicles, and so on. Based on this information, the system will decide whether the formation is acceptable for the current road conditions.

(2) The way the formation is generated will tell the unmanned vehicle system how to form the formation. For example, if the system requires a third geometric transformation to be performed for a convoy with the base formation of one row in the figure, then the convoy will move the outermost two vehicles backwards to the specified position to achieve this formation.

(3) The logic of the formation change determines the formation change idea of the fleet. For the formation change library in Figure 4, its formation change logic is as follows: firstly, the UGVs fleet receives external information and processes it to determine whether it needs to transform the formation geometry directly. If the condition of dynamic adjustment is satisfied, then dynamic adjustment takes priority, because dynamic adjustment has the least impact on the fleet and is easy to complete in a short time. Since the dynamic adjustment is achieved by scaling the distance between vehicles within the fleet, there is a limit to this scaling, i.e., the distance between vehicles cannot be smaller than the safe driving distance of the vehicles. When the limit of dynamic adjustment is reached, the fleet needs to change its strategy and select the appropriate formation in the library for geometry transformation.

After the transformation is completed, the fleet can still dynamically adjust the current formation until the road requirements are not met and the geometry transformation is continued.

Depending on the different mission requirements of UGVs fleets, the formation change library does not contain exactly the same formation types. Although the final geometries are not identical, the design ideas for performing formation changes are the same. It is worth noting that the goal of the formation change is to successfully negotiate complex terrains. Therefore, in practice, we designed the corresponding formation structure according to the common complex terrains, and further add or delete the convoy formation change methods in the library depending on the specific task requirements.

It is not enough to have a formation change library. The decision-making layer of the UGVs fleet system needs to analyze and process the external environmental information transmitted by the sensors before it can select the appropriate formation change in the formation change library to cope with more complex terrain and pass through it in the easiest and fastest way possible. These steps of analysis and processing represent the formation change impact factor.

2.3. Formation Change Influence Factor

The flexibility to cope with different complex terrains implies that the decision-making level of the UGVs fleet needs to have the ability to discriminate autonomously and determine the formation change plan of the fleet according to different external environments. Therefore, this paper proposes a formation change influence factor to influence vehicles to issue corresponding formation change commands.

In the traditional formation control, there is no autonomous formation change capability, and the formation change of the UGV fleet needs to be issued by humans. UGVs are usually equipped with sensors to identify the external environment and return information to the decision-making level of the system. Therefore, we assume that the vehicles in the unmanned fleet are equipped with distance detection devices, which can detect the distance from road boundaries and obstacles to the vehicles. Additionally, the intra-fleet communication between vehicles is good and the leader can obtain information about the individual follower poses. As in existing applications, UGVs fleets are commonly used by performing the corresponding tasks in structured terrain. Therefore, we describe how the formation change influence factor affects the formation change strategy of the UGVs fleet in two typical complex terrains.

2.3.1. Road Narrowing

Figure 5 indicates the narrowing of the road ahead. The UGVs fleet consists of one leader and four followers, with the blue dot representing the leader and the red dots representing the followers.

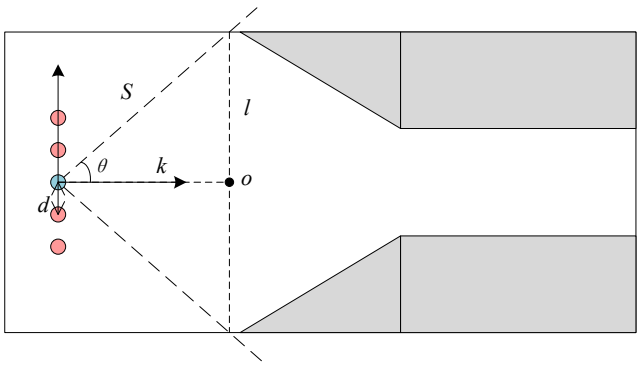

Figure 5. Road narrowing in front of the UGVs fleet.

The five vehicles move forward in a line, as shown in the figure. The width of each vehicle is e, the distance between vehicles is d, and the width of the fleet is $4d + e$. To ensure safe driving, we assume that the minimum distance between vehicles is d_m, then $d \geq d_m$. Assuming that the distance of the leader is far enough from the detection device, the maximum angle of the detection range is 2θ. With the forward direction of the fleet as the positive direction, the distance from the left road boundary to the leader at the maximum detection angle is S_l. According to the geometric relationship, the projection length of S_l in the vertical direction $l_l = S_l \sin\theta$, and the projection length in the positive direction $k_l = S_l \cos\theta$. Similarly, we can determine the projection length of the right road in each direction $l_r = S_r \sin\theta$, $k_r = S_r \cos\theta$.

Since formation change takes some time, for safety reasons, the fleet needs to perceive the road ahead and make judgments in advance, and the change of the road boundary affects the decision made by the leader. This influence is known as the formation change influence factor. It is a vector function influenced by the boundary distance, similar to the artificial potential field method, but it produces no force. To facilitate the representation, we choose to focus the influence effect of the factor at point o. The queue transformation decision factor is divided into two types. One of the types is the effect on the positive direction and the other is the effect on the vertical direction. Let the influence factor produced by the right road in the vertical direction be α_r and the influence factor produced by the left road be α_l; the influence factor produced by the right road in the positive direction be β_r and the influence factor produced by the left road be β_l. Then

$$\alpha_l = \begin{cases} K_1\left(\frac{1}{l} - \frac{1}{l_{l0}}\right)^{\frac{1}{2}}, & l \leq l_{l0} \\ 0 & , l \geq l_{l0} \end{cases} \tag{25}$$

$$\alpha_r = \begin{cases} K_1\left(\frac{1}{l} - \frac{1}{l_{r0}}\right)^{\frac{1}{2}}, & l \leq l_{r0} \\ 0 & , l \geq l_{r0} \end{cases} \tag{26}$$

$$\beta_l = \begin{cases} -K_2\frac{1}{k_l{}^2}, & l \leq l_{l0} \\ 0 & , l \geq l_{l0} \end{cases} \tag{27}$$

$$\beta_r = \begin{cases} -K_2\frac{1}{k_r{}^2}, & l \leq l_{r0} \\ 0 & , l \geq l_{r0} \end{cases} \tag{28}$$

In the above equation, K_1, K_2 are adjustable coefficients; $l_0(l_{l0}, l_{r0})$ is the farthest influence distance of the road boundary, when $l \leq l_0$, the road boundary will only have an influence on the vehicle, and the opposite means that the road is wide enough to allow the fleet, in the original formation, to pass safely; it also indicates the minimum road width without formation change. l_0 is usually determined by the width of the fleet. For the fleet in Figure 5, its fleet width on the left and right sides is $w_l = w_r$, then set $l_{l0} = w_l + d$, $l_{r0} = w_r + d$. In Figure 5, the road width is within the safe range, and the road boundary on both sides will not have an impact on the advance of the fleet; therefore, the fleet can keep the original formation and continue to advance.

When the fleet moves to the position in Figure 6, $l < l_0$, the road boundary starts to influence the UGVs fleet. Continuing to maintain the formation movement may lead to the occurrence of collision. The influence factors generated by the road boundaries on the left and right sides of the fleet are α_l and α_r, respectively, and they will jointly affect the overall angular velocity ω of the fleet. Additionally,

$$\omega = \omega_0 + A(\alpha_r - \alpha_l) \tag{29}$$

where ω_0 is the initial angular velocity of the fleet and A is the adjustable coefficient. According to Equation (25), the closer the road boundary is to the vehicle, the greater the impact on the vehicle. When the influence of one side of the road is greater, the angular

velocity of the fleet changes and the fleet starts to gradually move away from this side of the road until both sides of the road have the same influence or both have no influence. Similarly, as the road narrows, S becomes smaller, which leads to a reduction in both k and l. From Equation (26), it is clear that the road boundary has an impact factor β on the opposite direction of the fleet, which affects the overall line speed of the fleet, and

$$v = v_0 + B(\beta_r + \beta_l) \tag{30}$$

where v_0 is the initial angular velocity of the fleet and B is the adjustable coefficient. According to Equation (26), the smaller the width of the road, the greater the effect on the overall line speed of the fleet. The low speed into the complex terrain both provides the fleet with enough time to adjust the formation and ensures safer driving. To ensure that the fleet travels normally, this influence is limited to a certain extent; in other words, the fleet has a minimum speed, and when the influence factor β causes the overall line speed of the fleet to be lower than the minimum, the fleet will always travel at the minimum speed.

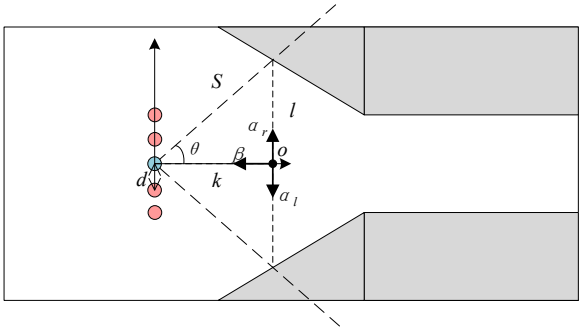

Figure 6. The impact of narrowing road boundaries on the UGVs fleet.

When the vertical influence factor α appears, it means that the road width no longer meets the requirement of maintaining the original formation for safe driving, and a formation change is needed. The priority of the formation change is to reduce the distance d by dynamic adjustment. At this point, the distance between vehicles is

$$d = d_0 - \frac{C}{2}|\alpha_r - \alpha_l| \tag{31}$$

where d_0 is the initial distance between vehicles and C is the adjustable factor. The variation of the vertical influence factor makes the distance between vehicles change continuously, but this change has a limit.

The width of the UGVs fleet cannot be reduced indefinitely. To ensure safe driving, a minimum distance d_m exists between vehicles. For the UGVs fleet in the figure, its minimum fleet width is $4d_m + e$, which is the limit distance that can be achieved by dynamic adjustment. When the fleet moves to the position in Figure 7, the road width is less than the minimum fleet width. For this case, the risk of collision between vehicles occurs by continuing with dynamic adjustment. When the road width is exactly $4d_m + e$, the influence factor of the road boundary in the vertical direction at this time is

$$\alpha_m = K_1 \left(\frac{1}{\left(2d_m + \frac{1}{2}e\right)} - \frac{1}{l_0} \right)^{\frac{1}{2}} \tag{32}$$

This means that the fleet needs to change the formation geometry when $(\alpha_r, \alpha_f) > \alpha_m$. According to each width of formation given by the formation change library, the appropriate formation geometry is selected from the largest to the smallest according to the prescribed logical relations.

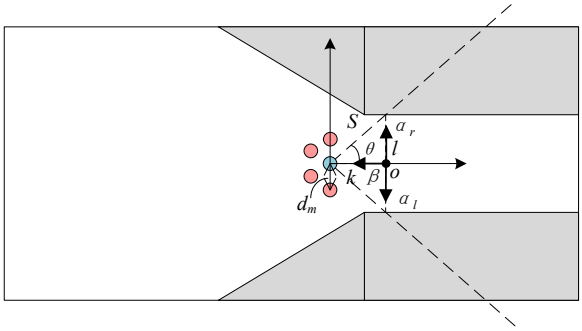

Figure 7. The impact of narrowed road boundaries on the UGVs fleet.

2.3.2. Road Obstruction

The second type of complex terrains is shown in Figure 8, where there is a partition, an obstacle or a fork in the road and other factors that force the fleet not to continue in its original formation. The blue dot indicates the leader and the red dots indicate the followers. The parameters for the UGVs fleet are the same as in the previous subsection. Usually, the fleet will set a safety zone ahead. When there is no obstacle ahead or the obstacle is far away, the fleet can move forward normally; when the obstacle is detected within the safety distance, it means the vehicle needs to make a decision to avoid the risk of collision. S_1, S_2 are the distances from the two ends of the obstacle to the leader detected by the leader distance detection device, and θ_1, θ_2 are the corresponding deflection angles. Taking the forward direction of the fleet as the positive direction, the projection length of S_1, S_2 in the vertical direction is

$$l_1 = S_1 \sin\theta_1 \tag{33}$$

$$l_2 = S_2 \sin\theta_2 \tag{34}$$

At this point, the widths of the channels on each side of the barrier are

$$W_1 = S\sin\theta - l_1 = S\sin\theta - S_1\sin\theta_1 \tag{35}$$

$$W_2 = S\sin\theta - l_2 = S\sin\theta - S_2\sin\theta_2 \tag{36}$$

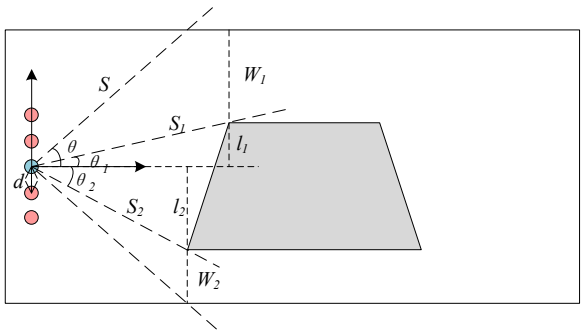

Figure 8. Road obstruction in front of the UGVs fleet.

According to the size of W_1 and W_2, we choose the appropriate formation in the formation change library. For the case where there are obstacles, if the widths of the passage on both sides are sufficient, we can choose to divide the fleet into two teams to pass on both sides. Following the transformation strategy outlined in Section 2.2, the fleet is divided into two sub-fleets, each with one leader. The newly generated leaders will keep their original linear and angular velocities moving forward until the formation change influence factors starts to work. Taking one of the sub-fleets as an example, Figure 9 provides the effect of the influence factors on the sub-fleet at this point.

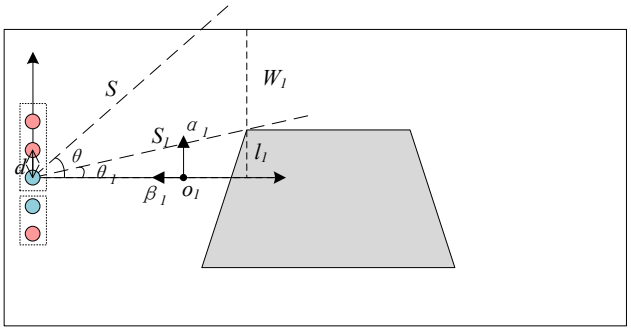

Figure 9. The impact of obstacles ahead on the UGVs fleet.

Since the sub-fleet consists of only 3 vehicles, the width of the left fleet is $w_l = 2d + 1/2e$, and the width of the right caravan is $w_r = 1/2e$. Accordingly, the farthest influence distances of the left and right roads on the sub-fleet are $l_{l0} = w_l + d$ and $l_{r0} = w_r + d$, respectively. At this time, the sub-fleet is much smaller than l_{l0} and l_{r0} from both sides of the road, so both sides of the road will not have an impact on the sub-fleet. Unlike the roads on both sides, the obstacles in front of the sub-fleet have an effect, and this effect also occurs in two directions. To facilitate the representation, we choose to concentrate the effect of the factors at the point o_1. Let the factor of the obstacle in the vertical direction be α_1 and in the positive direction be β_1, then

$$\alpha_1 = \begin{cases} K_3 {l_1}^2 & , l_1 > 0 \\ 0 & , l_1 \leq 0 \end{cases} \tag{37}$$

$$\beta_1 = -K_2 \frac{1}{(S_1 \cos\theta_1)^2} \tag{38}$$

α_1 and β_1 affect the overall angular velocity ω_1 and linear velocity v_1 of the sub-fleets, respectively, in the following manner:

$$\omega_1 = \omega_0 + A_1 \alpha_1 \tag{39}$$

$$v_1 = v_0 + B_1 \beta_1 \tag{40}$$

where ω_0 is the initial angular velocity of the sub-fleet, v_0 is the initial angular velocity of the sub-fleet, and A_1, B_1 are adjustable coefficients. According to Equation (35), the presence of l_1 will force the sub-fleet to move to the channel on the closer side. The smaller l_1 is, the smaller the influence of the obstacle on the sub-fleet. At the same time, the obstacle will also slow down the movement of the sub-fleet to avoid collision.

As the sub-fleet is offset, l_1 becomes smaller, and the influence of the obstacle on the sub-fleet diminishes. When l_1 decreases to 0, as shown in Figure 10, there is no obstacle directly in front of the sub-fleets. For the sub-fleet, the complex terrain has been transformed from an obstacle blockage to road narrowing. In the manner of the previous subsection, the factors α_{1l}, α_{1r} and β generated on both sides of the road start to influence the sub-fleet's decision to choose dynamic adjustment or to select the appropriate formation structure for change in the formation change library. When passing the obstacle section, the fleet reverts to the original formation.

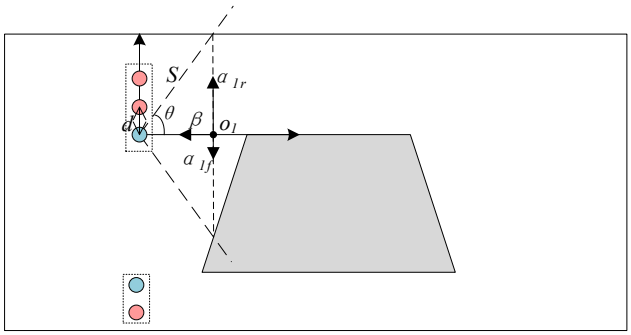

Figure 10. The impact of road boundaries on the UGVs fleet after moving away from the obstacle.

With two common complex terrains, this paper provides the operation mode of the formation change influence factor. With the intervention of the factor and the formation change library, the fleet can flexibly choose the appropriate formation change according to the complex terrains encountered. In addition, the influence factor also controls the overall speed of the fleet, thus ensuring stability and safety during the formation change.

By designing a formation change library and formation change influence factor and combining the two, this paper proposes a new unmanned ground vehicle formation and change method, which ensure that the UGVs fleet has the ability to flexibly cope with the complex terrains encountered during the movement. Compared with the traditional UGVs formation method, this method has stronger adaptability and a better problem handling mechanism, which further improves the safety, stability and practical application capability of the UGVs fleet.

3. Simulation Experiments

In this section, the simulation experiments for each part of the Section 2 will be provided. First, the UGVs formation controller under the leader–follower method will be tested and simulation results will be detailed to illustrate its stability; after that, simulation experiments will be outlined to implement the UGVs formation change using the formation change influence factor. This experiment is divided into two different experiments to show the experimental results under two different complex terrains. The feasibility of the method is demonstrated by comparing the variations of each parameter.

3.1. The UGVs Formation Controller

As one of the traditional formation control methods, the leader–follower method has become the most commonly used formation control method with the advantages of more flexible control and easier formation construction. Assume that the UGVs fleet consists of five identical UGVs, all with the vehicle model shown in Figure 1. One of them is chosen as the leader and the remaining four as the followers. The relevant parameters of the vehicles and fleet are shown in Table 1.

Table 1. The relevant parameters in the formation controller test.

Leader Initial Position	Number of UGVs	Vehicle Width	Distance between Vehicles	Maximum Vehicle Line Speed
(20,20) m	5	2 m	5 m	5 m/s
Leader Initial Line Speed	**Leader Initial Angular Velocity**	**Leader Initial Direction Angle**	**l_x' of the Initial Fleet**	**l_y' of the Initial Fleet**
5	0 rad/s	0 rad	[0, 0, 0, 0] m	[−5, −10, 5, 10] m

The initial positions of the vehicles are shown in Figure 11a, where the blue dot indicates the leader, the red dots indicate the followers and the number next to the red dots represents the follower numbers. The expected formation of the UGVs formation is shown

in Figure 11b. The followers are symmetrically distributed in a row on both sides of the leader and always maintain this formation during movement.

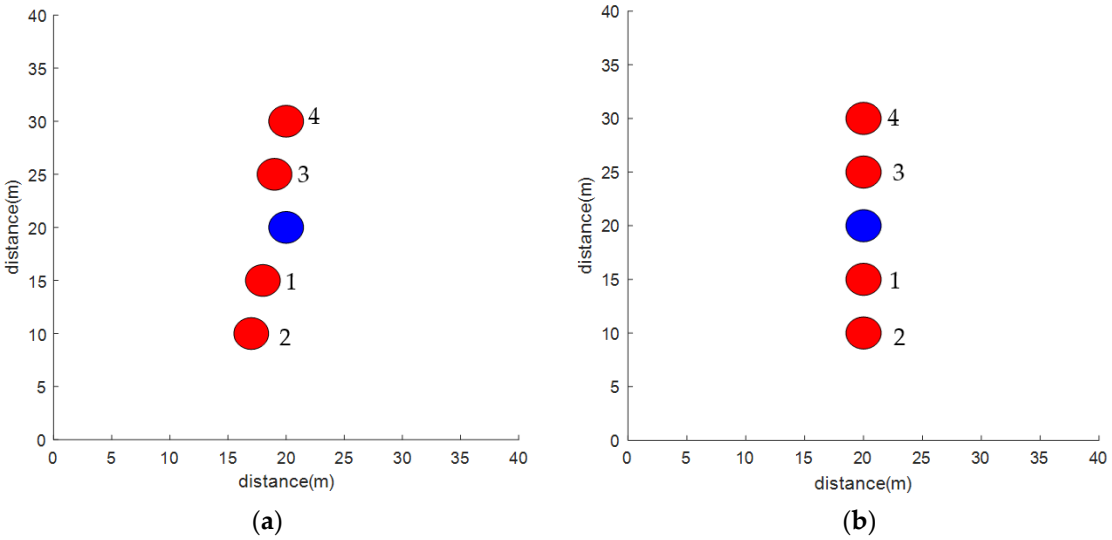

Figure 11. Initial position and expected formation of each vehicle in the UGVs fleet. (**a**) indicates initial positions of the vehicles and (**b**) indicates the expected formation of the fleet.

The leader moves according to a pre-defined S-shaped route. Figure 12 below demonstrates the overall trajectory of the fleet.

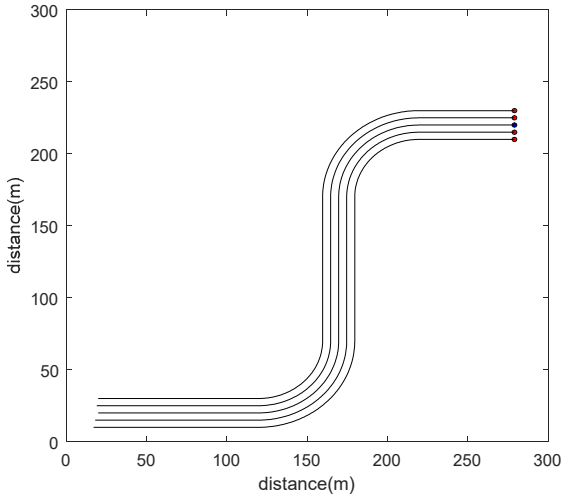

Figure 12. The fleet trajectory under the leader–follower formation controller.

It can be seen that the controller given in Section 2.1 achieves good results in terms of the UGVs formation. Even when making a turn, the fleet can still maintain the expected formation. The variation curves of l_x, l_y and e_θ for each follower during the movement of the UGVs fleet along the above route and parameter conditions are given below.

As can be seen from Figures 13–15, after a short period of time, the followers successfully reach their designated positions and maintain their relative positions in co-movement with the leader during the subsequent process. Accordingly, both the l_x and l_y of each follower remain stable at the desired values after the fleet in the expected formation. In contrast, e_θ gradually stabilizes at a fixed value after starting to increase at two turns. At the end of the turns, e_θ returns to 0. Since the overall fluctuation of e_θ is not significant, the fleet remains stable as a whole. To better illustrate the effect of the controller, the variation curves

of the linear and angular velocities of the leader and the followers during the movement are given in Figures 16–19.

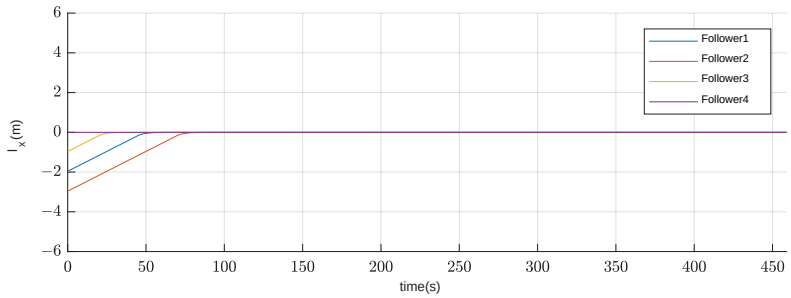

Figure 13. The variation curves of l_x for each follower during the movement.

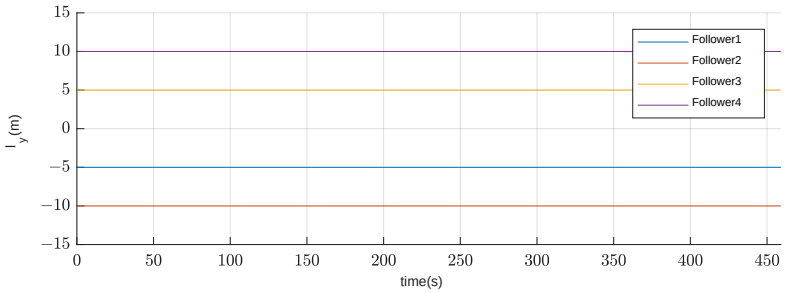

Figure 14. The variation curves of l_y for each follower during the movement.

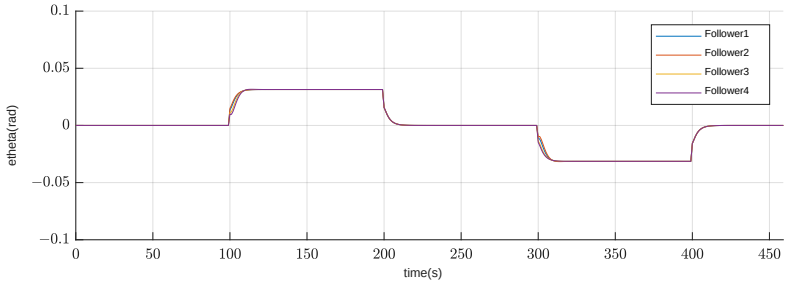

Figure 15. The variation curves of e_θ for each follower during the movement.

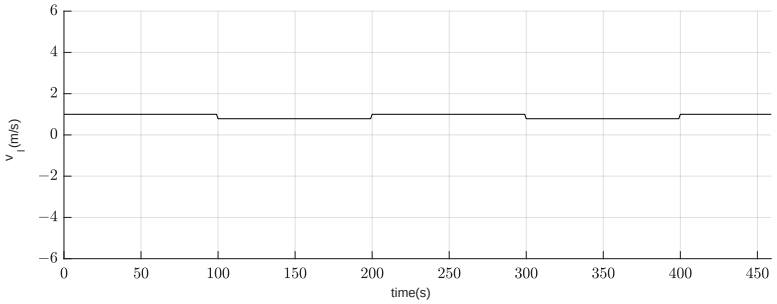

Figure 16. The variation curve of v_l for the leader during the movement.

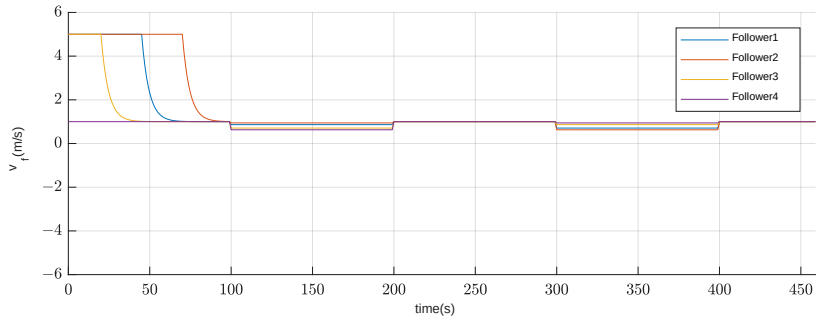

Figure 17. The variation curves of v_f for each follower during the movement.

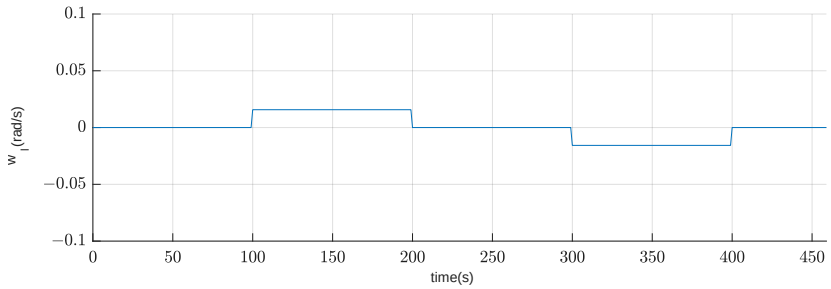

Figure 18. The variation curve of ω_l for the leader during the movement.

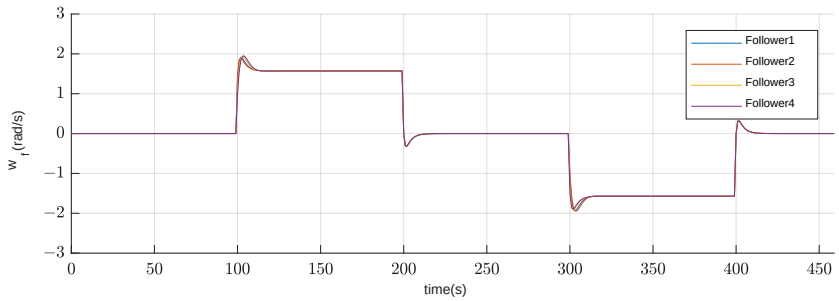

Figure 19. The variation curves of ω_f for each follower during the movement.

When the leader keeps moving in a straight line, its linear velocity v_l is kept at an initial fixed velocity of 1 m/s; when it starts to turn, v_l decreases appropriately. The fact that the followers are not in their expected positions before the UGVs fleet movement and the leader has an initial speed makes the distances between the followers and the leader increase when the fleet starts moving. Therefore, the followers start with a higher linear velocity v_f through the controller to reduce the distances to the desired positions, and then gradually reduce their velocity to reach the desired position, where v_f is aligned with v_l. The time taken for this process varies depending on the initial position.

As the fleet begins to turn, v_f decreases accordingly, with vehicles near the inside of the curve slowing down less and vice versa, so as to keep the overall formation constant. Similarly, the angular velocity ω_l of the leader will increase toward the turn, while the follower angular velocity ω_f increases slightly more while maintaining the trend of ω_l; however, the overall fleet still remains stable.

It can be seen from the above experimental results that the formation controller imparts an excellent effect on the UGVs' formation, proving its stability and reliability.

3.2. Road Narrowing

Due to the advantages of the leader–follower method, it is easier to implement both dynamic adjustment and geometric transformation for the UGVs fleet. Therefore, after obtaining a stable and effective formation controller, the experimental results of the UGVs

formation transformation under the influence of formation transformation factors are presented based on this paper.

Firstly, we simulate the formation transformation under the condition of the road narrowing. It is assumed that the UGVs fleet consists of five identical UGVs, each with the same configuration. All vehicles can be leaders, and the fleet adopts the formation controller given in Section 2.1. Table 2 provides the relevant parameters for the UGVs fleet, the map environment and changing the formation.

Table 2. The relevant parameters in case of road narrowing.

Number of UGVs	**Vehicle Width**	**Distance between Vehicles**	$l_x{}'$ **of the Initial Fleet**	$l_y{}'$ **of the Initial Fleet**
5	2 m	5 m	[0, 0, 0, 0] m	[−5, −10, 5, 10] m
Leader Initial Position	**Leader initial line speed**	**Leader initial angular velocity**	**Leader Initial Direction angle**	**Maximum vehicle line speed**
(5,40) m	2 m/s	0 rad/s	0 rad	5 m/s
Maximum road width	**Minimum road width**	**Minimum distance between vehicles**	$l_x{}'$ **of the changed fleet**	$l_y{}'$ **of the changed fleet**
80 m	12 m	3 m	[0, −5, 0, −5] m	[−3, −1.5, 3, 1.5] m
K1	**K2**	**A**	**B**	**C**
1	2	0.0062	0.55	1

Figure 20 presents a map of the road narrowing and the result of the path of the fleet under this map.

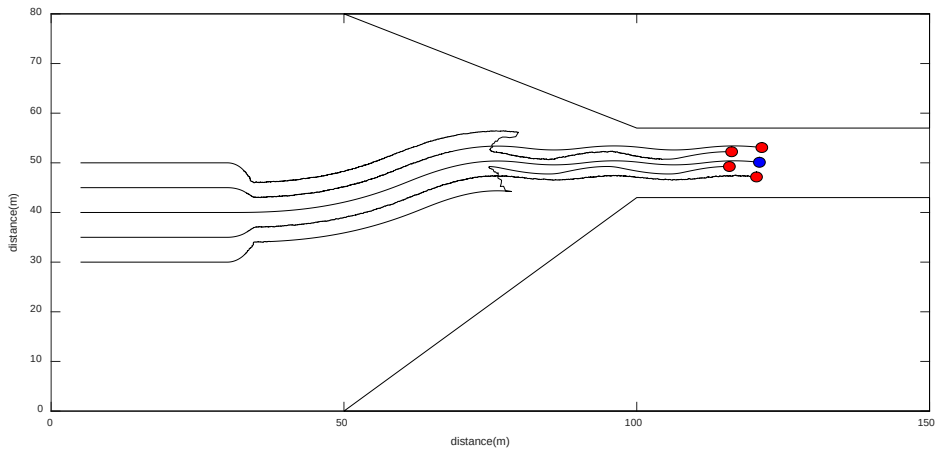

Figure 20. Trajectory of the UGVs fleet in the case of road narrowing ahead.

It can be seen that in the initial stage the fleet keeps the preset formation moving forward. When it is detected that the road ahead is unable to maintain the current distance between vehicles safely, the fleet starts to tighten the fleet width to ensure passing through due to the effect of formation change influence factors. Continuing forward, the fleet finds that the road continues to narrow. At this point, the factors are higher than the maximum limit, and continuing to tighten the fleet will cause the distance between the vehicles to fall below the minimum distance. Therefore, the fleet starts to continue to reduce the width by changing the geometry of the fleet according to the logical relations determined by the formation change library. Eventually, the UGVs fleet is able to pass the narrow road safely.

When entering the narrow section, the fleet trajectory oscillates to a certain extent because of the smaller distance between the two sides of the road and the fleet, and the oscillation of the rear vehicles is more obvious due to the formation. Since this paper

presents a kinematic model of the UGV for control rather than a kinetic model, this makes the fleet as a whole more sensitive to changes in linear and angular velocities and prone to oscillations. However, the magnitude of this oscillation is small and does not exceed the width of the UGV itself. Again, in practice, the slight oscillation of the fleet will not affect the inability to pass narrow sections of road, so this phenomenon is within acceptable limits.

Since the leader is the decision center of the UGVs fleet and the direct object of the formation change influence factor, Figures 21–23 provide the changes of the linear velocity v_l, angular velocity ω_l and direction angle θ_l of the leader throughout the movement. The overall change trend of the followers is the same as that of the leader due to the presence of the formation controller. In the initial stage, the fleet keeps the original v_l, ω_l and θ_l moving forward. When narrowing of the road is detected, the fleet moves away from the road boundary on the closer side under the influence factor, ω_l starts to increase, and θ_l also starts to change. When the fleet gradually approaches the entrance of the narrow passage, ω_l decreases and θ_l reverses, and finally stabilizes in a small range of variation. As part of this process, v_l also decreases due to the narrowing of the road, and finally tends to change smoothly.

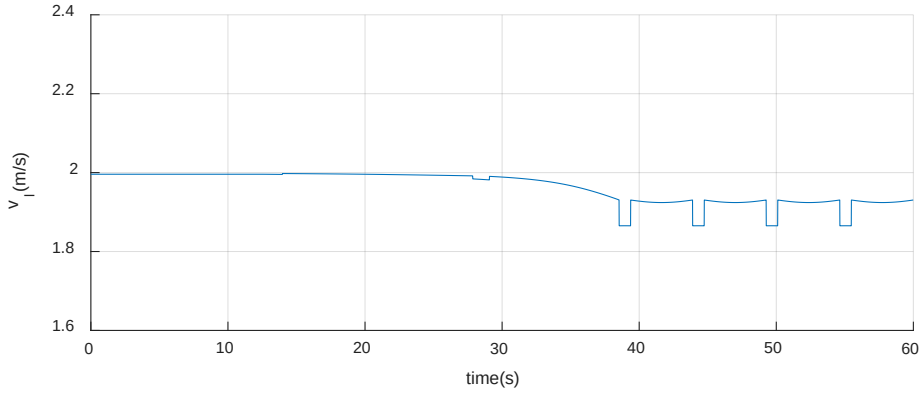

Figure 21. The variation curve of v_l for the leader during the movement.

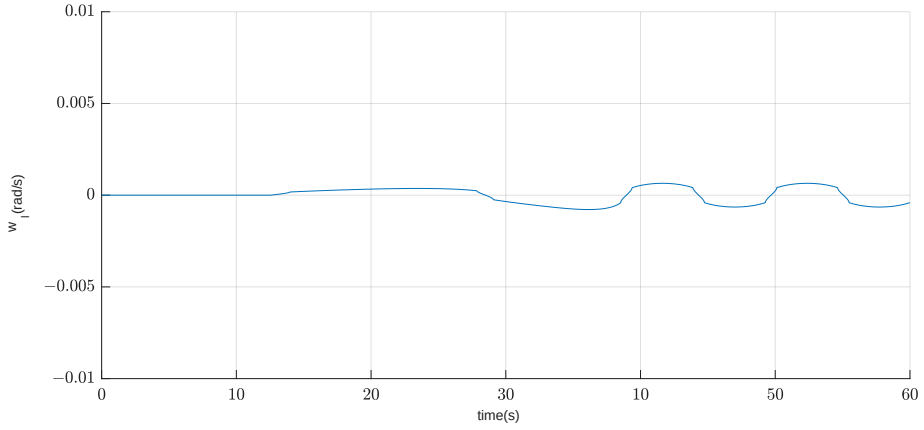

Figure 22. The variation curve of ω_l for the leader during the movement.

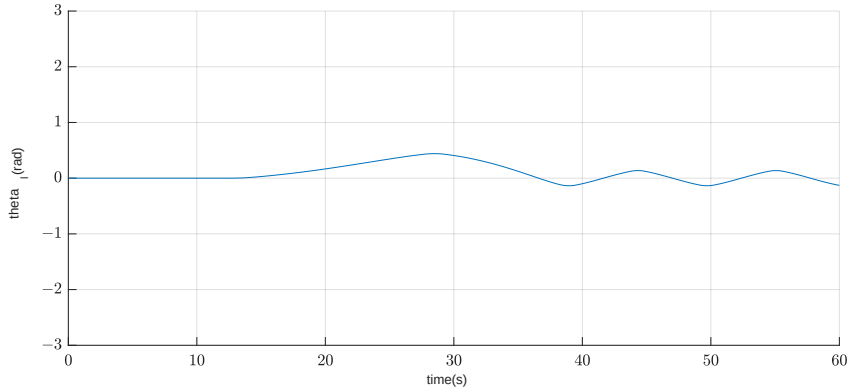

Figure 23. The variation curve of θ_l for the leader during the movement.

Figures 24 and 25 illustrate the variation of the relative distances l_x and l_y between the followers and the leader. The specific changes in the formation during the movement, including the transition from dynamic adjustment to geometric transformation, can be seen in these results.

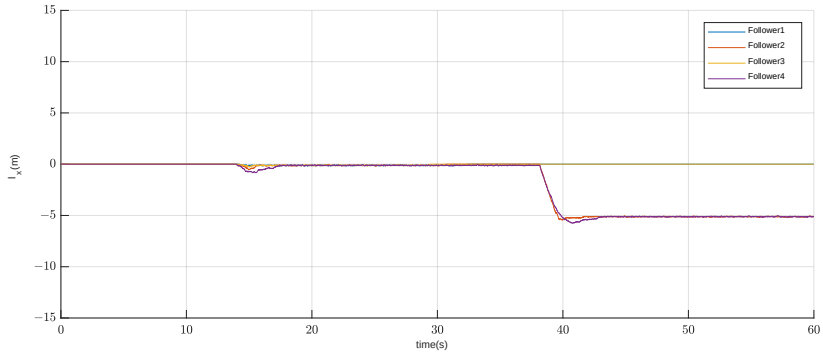

Figure 24. The variation curves of l_x for each follower during the movement.

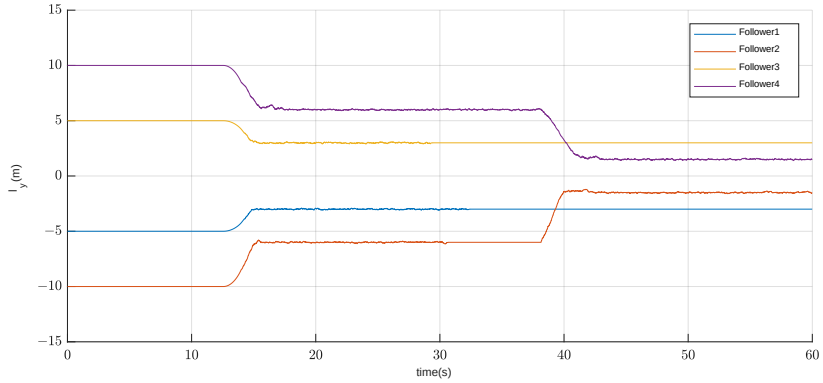

Figure 25. The variation curves of l_y for each follower during the movement.

3.3. Road Obstruction

Next is the simulation experiment of formation change in case of road obstacles. Compared to road narrowing, this terrain is more complex and will require a greater level of decision making and control of the fleet. It is assumed that the UGVs fleet consists of five identical UGVs, each with the same configuration, all of which can be leaders, and the fleet uses the formation controller described in the previous section. Table 3 details the parameters related to the UGVs fleet, the map environment and the changing formation.

Table 3. The relevant parameters in case of road obstruction.

Number of UGVs	**Vehicle Width**	**Distance between Vehicles**	$l_x{}'$ **of the Initial Fleet**	$l_y{}'$ **of the Initial Fleet**
5	2 m	5 m	[0, 0, 0, 0] m	[−5, −10, 5, 10] m
Leader Initial Position	**Leader Initial Line Speed**	**Leader Initial Angular Velocity**	**Leader Initial Direction Angle**	**Maximum Vehicle Line Speed**
(5,40) m	2 m/s	0 rad/s	0 rad	5 m/s
Maximum road width	**Minimum Road Width**	**Minimum Distance between Vehicles**	$l_x{}'$**of the Changed Fleet**	$l_y{}'$**of the Changed Fleet**
80 m	18 m/15 m	3 m	[0, 0] m and 0 m	[5, 10] m and −5 m
K1	**K2**	**A**	**B**	**C**
1	2	0.006	0.545	1

Figure 26 details the map in case of a road obstacle and the result of the fleet's path under this map.

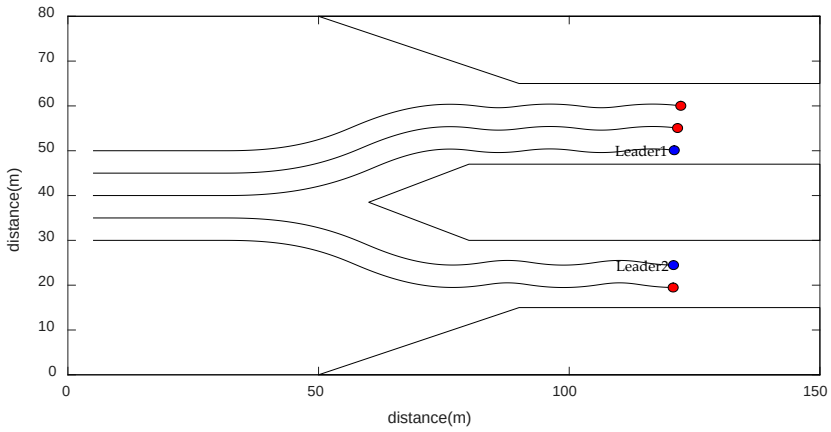

Figure 26. Trajectory of the UGVs fleet in the case of road obstruction ahead.

In the initial stage the fleet moves forward in a preset formation. When an obstacle is detected on the road ahead, the decision layer chooses to change the formation geometry according to the logical relationships in the formation transformation library, and divides the fleet into sub-fleets consisting of 3 vehicles and 2 vehicles, respectively. The two sub-fleets are affected by the formation transformation influence factor generated by the obstacle and start to gradually approach the passages on both sides of the obstacle. Continuing to move forward, the fleet found that the road continued to narrow. Under the influence factor, the influence from the obstacle gradually decreases until it disappears; while the influence from the road on both sides drives the sub-fleets to enter the passages on both sides of the obstacle at a safe angle and distance.

After splitting into two sub-fleets, each group of fleets will have one leader each. Figures 27–29 outline the changes of linear velocity v_l, angular velocity ω_l and direction angle θ_l of the two leaders during the whole moving process. In the initial stage, the fleets move forward with the original v_l, ω_l and θ_l. When an obstacle is detected on the road, the fleets move to each side of the obstacle due to the influence factor, ω_l starts to increase, and θ_l also starts to deflect. When the fleets gradually approach the entrance of the narrow passage, ω_l decreases and θ_l slews, and finally stabilizes in a small range of variation. In this process, v_l also decreases continuously due to the narrowing of the road, and finally tends to change smoothly.

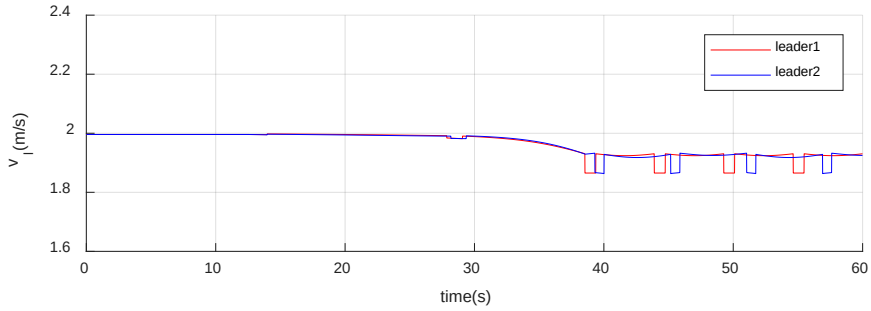

Figure 27. The variation curves of v_l for the leaders during the movement.

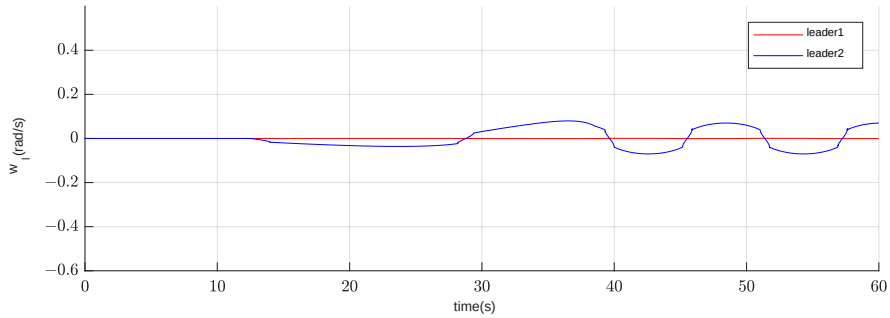

Figure 28. The variation curves of ω_l for the leaders during the movement.

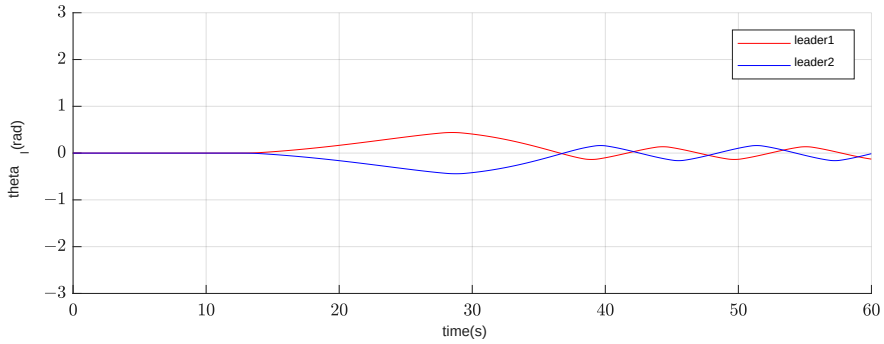

Figure 29. The variation curves of θ_l for the leaders during the movement.

Since the sub-fleets are differentiated from the original fleet, the controller parameters of the fleet remain the same as the original. However, the sub-fleets have changed in fleet size and structure compared with the original fleet, and the original parameters may not be able to better match the current sub-fleets control. Combined with the kinematic model, this also explains the fluctuation of ω_l in Figure 28. However, the overall fluctuations are small and have little impact on the fleets running and are within the acceptable range.

Figures 30 and 31 express the variation of the relative distances l_x and l_y between the followers and the leader of each sub-fleet. The specific changes in the formation during the movement can be seen in these results. It shows that the stability within the fleet can still be maintained during the movement.

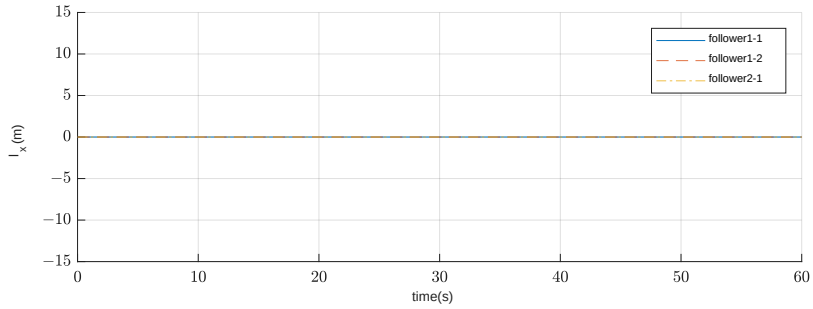

Figure 30. The variation curves of l_x for each follower during the movement. Follower 1-1 indicates the position of follower No.1 in sub-fleet No.1, and follower 2-1 indicates the position of follower No.1 in sub-fleet No.2.

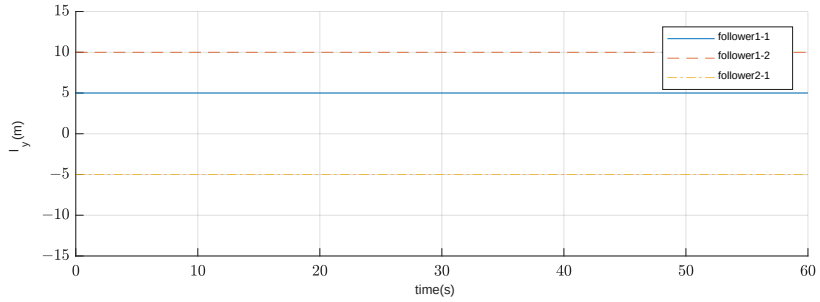

Figure 31. The variation curves of l_y for each follower during the movement. Follower 1-1 indicates the position of follower No.1 in sub-fleet No.1, and follower 2-1 indicates the position of follower No.1 in sub-fleet No.2.

4. Conclusions

In this paper, we propose formation change influence factors to solve the unmanned fleet formation and formation change problem. Since the traditional formation control method lacks a mechanism by which to effectively deal with the complex road conditions that occur during the movement, the perspective of formation change is used to manage this. First, this paper adopts the leader–follower method with more flexible control to design the formation controller. Using the input-output linearization method, a control law that can make the UGVs formation system stable is derived to ensure that the fleet always maintains the preset formation during the movement. Based on this controller, we propose a formation change influence factor and a formation change library to provide the UGVs fleet with the ability to change formation flexibly according to the complex terrains ahead. Different formation geometries and dynamic adjustment methods that may be required are added to the formation change library, and the formation change logic is determined. Afterwards, the formation change influence factor for different terrain is generated by the terrain ahead obtained from the distance detection device of the fleet, and this influences the overall line speed and angular speed of the fleet to ensure that the fleet can pass the complex terrain safely.

The experimental results show that the UGVs fleet can flexibly and effectively cope with complex terrains under the influence factor of formation change. When the road becomes narrower or obstacles appear, the fleet can flexibly adjust the formation structure according to the terrain to ensure that the fleet passes the terrain safely, which is difficult to achieve for the traditional formation methods. At the same time, the new formation and change method proposed in this paper can also maintain the internal stability of the UGVs fleet, which effectively improves the safety of the UGVs fleet operation and the possibility of application in practice.

Because we assume a vehicle model with perfect speed control, only the kinematic model of the vehicle is considered in this paper, not the dynamics model. In addition, this paper only details experiments for applications in two structured terrains. For other

different terrains, the formation change library can be further updated according to the terrain characteristics. How to cope with unstructured terrain during formation change and how to solve the slight oscillation of the convoy forward route caused by narrow road sections are topics for future research.

Author Contributions: Conceptualization, T.G. and J.S.; methodology, T.G.; software, T.G.; validation, J.S.; writing—original draft preparation, T.G. and J.S.; writing—review and editing, T.G. and Y.Y.; supervision, Y.Y.; funding acquisition, J.S. All authors have read and agreed to the published version of the manuscript.

Funding: This research was supported by National Program on Key Research Project of China under Grant 2017YFC0821001, Shenyang Young and Middle-aged Science and Technology Innovation Talent Support Program RC210247 and Liaoning Provincial Department of Education Basic Research Projects for Higher Education Institutions LJKZ0275.

Data Availability Statement: Not applicable.

Conflicts of Interest: The authors declare no conflict of interest regarding the publication of this manuscript.

References

1. Mohamed, A.K.; Xiang, Y.; Youmin, Z. Formation control and coordination of multiple unmanned ground vehicles in normal and faulty situations: A review. *Annu. Rev. Control.* **2020**, *49*, 128–144.
2. Renhui, H.; Xiangjun, Z.; Kunyan, U.; Xianzhang, W. Development Status, Characteristics and Trends of Military Unmanned Vehicles for Foreign Military. *Automot. Appl.* **2011**, *8*, 21–22.
3. Zhang, Y.; Mehrjerdi, H. A survey on multiple unmanned vehicles formation control and coordination: Normal and fault situations. In Proceedings of the 2013 International Conference on Unmanned Aircraft Systems (ICUAS), Atlanta, GA, USA, 28–31 May 2013.
4. Yang, L.; Jia, Y. An iterative learning approach to formation control of multi-agent systems. *J. Syst. Control. Lett.* **2012**, *61*, 148–154.
5. Giroung, L.; Dongkyoung, C. Decentralized behavior-based formation control of multiple robots considering obstacle avoidance. *Intell. Serv. Robot.* **2018**, *11*, 127–138.
6. Sida, L.; Ruiming, J.; Ming, Y.; Yuan, X. On Composite Leader–follower Formation Control for Wheeled Mobile Robots with Adaptive Disturbance Rejection. *Appl. Artif. Intell.* **2019**, *33*, 1–21. [CrossRef]
7. Park, B.S.; Yoo, S.J. Connectivity-maintaining obstacle avoidance approach for leader-follower formation tracking of uncertain multiple nonholonomic mobile robots. *Expert Syst. Appl.* **2021**, *171*, 114589. [CrossRef]
8. Zhi, Y.C.; Gu, Y.H.; Long, I.; Xu, X.L. Unmanned vehicle formation method based on improved pigeon flock algorithm and pilot following method. *J. Machine Tools and Hydraulics.* **2022**, *50*, 25–31.
9. Wang, X.S.; Cao, G.H. Formation control of unmanned vehicles with multiple unknowns. *J. Vehicle and Power Technology.* **2019**, *2*, 43–47.
10. Shao, J.; Shi, L.; Cheng, Y.; Li, T. Asynchronous Tracking Control of Leader-Follower Multiagent Systems With Input Uncertainties Over Switching Signed Digraphs. *IEEE Trans. Cybern.* **2021**, *52*, 6379–6390. [CrossRef]
11. Shoja, S.; Baradarannia, M.; Hashemzadeh, F.; Badamchizadeh, M.; Bagheri, P. Surrounding control of nonlinear multi-agent systems with non-identical agents. *ISA Trans.* **2017**, *70*, 219–227. [CrossRef]
12. Ali, Z.A.; Israr, A.; Alkhammash, E.H.; Hadjouni, M. A Leader-Follower Formation Control of Multi-UAVs via an Adaptive Hybrid Controller. *Complexity* **2021**, *2021*, 9231636. [CrossRef]
13. Li, D.; Ge, S.S.; He, W.; Ma, G.; Xie, L. Multilayer formation control of multi-agent systems. *Automatica* **2019**, *109*, 108558. [CrossRef]
14. Wang, B.; Ashrafiuon, H.; Nersesov, S. Leader–follower formation stabilization and tracking control for heterogeneous planar underactuated vehicle networks. *Syst. Control Lett.* **2021**, *156*, 105008. [CrossRef]
15. Liu, X.; Ge, S.S.; Goh, C.H. Formation Potential Field for Trajectory Tracking Control of Multi-Agents in Constrained Space. *Int. J. Control.* **2017**, *90*, 2137–2151. [CrossRef]
16. Sang, H.; You, Y.; Sun, X.; Zhou, Y.; Liu, F. The hybrid path planning algorithm based on improved A* and artificial potential field for unmanned surface vehicle formations. *Ocean Eng.* **2021**, *223*, 108709. [CrossRef]
17. Raghuwaiya, K.; Sharma, B.; Vanualailai, J. Leader-Follower Based Locally Rigid Formation Control. *J. Adv. Transp.* **2018**, *2018*, 1–14. [CrossRef]
18. He, S.; Wang, M.; Dai, S.-L.; Luo, F. Leader–Follower Formation Control of USVs With Prescribed Performance and Collision Avoidance. *IEEE Trans. Ind. Inform.* **2018**, *15*, 572–581. [CrossRef]

19. Tao, P.; Shan, L. Formation control of multiple wheeled mobile robots via leader-follower approach. In Proceedings of the 26th Chinese Control And Decision Conference (2014 CCDC), Changsha, China, 31 May–2 June 2014.
20. Li, X.; Xiao, J.; Tan, J. Modeling and Controller Design for Multiple Mobile Robots Formation Control. In Proceedings of the 2004 IEEE International Conference on Robotics & Biomimetics, Shenyang, China, 22–26 August 2004.
21. Mehrjerdi, H.; Ghommam, J.; Saad, M. Nonlinear coordination control for a group of mobile robots using a virtual structure. *Mechatronics* **2011**, *21*, 1147–1155. [CrossRef]
22. Neto, V.E.; Sarcinelli-Filho, M.; Brando, A.S. Trajectory-tracking of a Heterogeneous Formation Using Null Space-Based Control. In Proceedings of the 2019 International Conference on Unmanned Aircraft Systems (ICUAS), Atlanta, GA, USA, 11–14 June 2019.
23. Moreira, M.; Brandao, A.S.; Sarcinelli-Filho, M. Null Space Based Formation Control for a UAV Landing on a UGV. In Proceedings of the 2019 International Conference on Unmanned Aircraft Systems (ICUAS), Atlanta, GA, USA, 11–14 June 2019.
24. Zhou, S.; Hua, Y.; Dong, X.; Ling, Q.; Ren, Z. Air-Ground Time Varying Formation Tracking Control for Heterogeneous UAV-UGV Swarm System. *J. Aero Weaponry.* **2019**, *26*, 54–59.
25. Tran, V.P.; Garratt, M.A.; Petersen, I.R. Switching formation strategy with the directed dynamic topology for collision avoidance of a multi-robot system in uncertain environments. *IET Control. Theory Appl.* **2020**, *14*, 2948–2959. [CrossRef]
26. Allam, A.; Nemra, A.; Tadjine, M. Parametric and Implicit Features-Based UAV–UGVs Time-Varying Formation Tracking: Dynamic Approach. *Unmanned Syst.* **2021**, *10*, 109–128. [CrossRef]